Zhang *et al. Geothermal Energy* (2023) 11:31
https://doi.org/10.1186/s40517-023-00274-2

Geothermal Energy

RESEARCH Open Access

Study on permeability evolution and damage mechanism along the EGS fracture in heat mining stage under thermal stress/cracking

Wei Zhang[1,2,3*], Dong Wang[2], Zenglin Wang[2,3], Tiankui Guo[3], Chunguang Wang[1], Jiayuan He[4], Le Zhang[4], Peng Zheng[5] and Zhanqing Qu[3]

*Correspondence: zhwei1990@sdust.edu.cn

[1] College of Energy and Mining Engineering, Shandong University of Science and Technology, Qingdao 266590, China
[2] New-Energy Development Center of Shengli Oilfield, Sinopec, Dongying 257051, China
[3] Key Laboratory of Unconventional Oil & Gas Development (China University of Petroleum (East China)), Ministry of Education, Qingdao 266580, People's Republic of China
[4] Sinopec Petroleum Exploration and Production Research Institute, Beijing 100083, China
[5] Qingdao Wofu New Energy Science and Technology Co.,Ltd, Qingdao 266010, China

Abstract

As main heat exchange channel in enhanced geothermal system, the evolution of hydraulic conductivity in fracture is significance for efficient heat mining. For the thermal stress or thermal cracking spontaneously induced by the temperature difference between low-temperature fluid and hot rock in heat mining stage, it is necessary to explore the damage mechanism along EGS fracture and the corresponding permeability evolution. Firstly, the long-term permeability tests under high temperature (50–200 ℃) were conducted by the self-developed high temperature seepage experimental device. Then, a coupled THM-D model was constructed to describe the damage distribution along fracture. Combined with experimental and simulation results, relationship between the thermal stress/cracking and the evolution of fracture permeability is revealed. The results indicate that during high-temperature (200 ℃) experiments, the fracture permeability first increases rapidly under the low-temperature induced thermal stress/cracking, then decreases due to the blockage effect induced by the debris particles generated in thermal cracking along fracture. The enhancement of injection velocity and heterogeneity are all conducive to the emergence of thermal cracking in matrix along fracture. Simultaneously, high confining pressure has a negative effect on the migration of debris particles of thermal cracking, which contribute to prevent the blockage of debris particles.

Keywords: Enhanced geothermal system, High temperature fracture permeability, Thermal stress, Thermal cracking, Damage simulation

Introduction

Geothermal energy has the advantages of green, stable, rich resources and renewable, comparing with the fossil energy such as coal, oil and gas. The hot dry rock located in deep part of the earth is rich in high temperature heat energy, but the characteristics of large buried depth and low permeability make it difficult to extract the high temperature resource to ground for human use (César et al. 2014; Xin et al. 2012). Enhanced geothermal system (EGS) is a key technology for efficient development of hot dry rock (HDR),

which indicate the use of fracturing technology to create artificial fractures or improve the original fractures to enhance the seepage feature in hot reservoir, and the extraction of geothermal energy is realized by the circulating of heat carrying medium. Meanwhile, based on the construction of EGS, it can effectively improve the mass flow rate and accumulated heat recovery to meet the requirements of geothermal power generation and comprehensive utilization (Hofmann et al. 2014a, b). As the main heat exchange channels of heat carrying medium, the effective formation and the conductivity evolution of artificial fractures are of great significance for heat extraction in HDR development (Zinsalo et al. 2021; Ma et al. 2020a, b).

Regarding the heat mining performance and the evolution of fracture conductivity in EGS, scholars have carried out a lot of research. Bujakowski et al. (2015), Zeng et al. (2013) and Zhang et al. (2015) applied TOUGH2 to evaluate the heat recovery of hot reservoir, the results showed that the volume and the permeability of stimulated zone have the significant impact on EGS exploitation. Jeanne et al. (2014) used a THM (thero-hydro-mechanical) coupling model to investigate the influence of injection pressure and thermal stress on EGS development, the results showed that under the co-function of injection pressure and thermal stress micro-crack may generate around the main fracture, then the damaged zone will further affect the heat mining performance. Zhao et al. (2015) conducted the THM coupling simulation and drawn the conclusion that the heat extraction efficiency will be improved by lowering the flow resistance in EGS, then gradually decreases with the operation time. Xiong et al. (2013) established THCM (thero-hydro-chemical–mechanical) coupling model to simulate the EGS production, and concluded that the rock deformation and chemical reaction during heat mining can influence the production rate by controlling the permeability. Bongole et al. (2021), Qu et al. (2017) and Jiang et al. (2014) studied the heat mining rate when using water and $SCCO_2$ (supercritical CO_2) as heat carrying medium, and the results showed that the development span is longer when water is used and the heat recovery rate is higher when $SCCO_2$ is used (The outlet temperature of EGS needs to be kept above a certain temperature. When it is reduced below this temperature, it has no development value. So we define the development time from the initial state of EGS development to the temperature with no development value as the development span.). Guo et al. (2020) used the analytic hierarchy and fuzzy comprehensive evaluation method to evaluate the heat recovery performance in EGS under different development schemes. Li et al. (2021) and Zhang et al. (2019a, b) based on the discrete fracture network discussed the influence of well-layout pattern and fracture feature on heat mining rate. Shu et al. (2019) conducted long core seepage capacity tests with a single fracture for the duration of 27 h, and found that the fracture conductivity decreases with the increase of operation time under the function of mineral dissolution, precipitation and rock damage. Zhao et al. (2020) and Avanthi et al. (2019) carried out experimental research on the interaction between granite and different water type, the results showed that even at a temperature of 150 ℃ and a pressure of 8 MPa, the reaction time of water-HDR reaction still needs more than 24 h.

The EGS reconstruction is to form some seepage channels in the hot reservoir by means of reservoir stimulation such as artificial fracturing, thus providing the channels for heat transfer. In the reconstruction of HDR, tensile cracks are formed in tight reservoir and shear slip occur in reservoir with natural fractures. Nadimi et al. (2020) and

Sheng et al. (2020) explored the rule of fracture slip induced by water injection in HDR with original fracture, they found that the contribution of thermal stress to the reduction of effective stress can reach 40%. Kumari et al. (2018), Li et al. (2021) and Zhang et al. (2019a, b) investigated the cracking process of intact high-temperature granite, the results showed that the low-temperature induced thermal stress caused by temperature difference between the injection fluid and the hot rock has a significance influence on the formation of multiple fracture in thermal reservoir. In addition, according to the characteristics of thermal cracking in hot rocks, zhang et al. (2021) tried to use cryogenic liquid CO_2 and Huang et al. (2020) and Li et al. (2018) tried to use liquid nitrogen to complete high-efficiency fracturing in HDR. It can be seen that the effect of thermal stress and thermal cracking cannot be ignored for HDR fracturing.

For the mechanism and influencing factors of thermal stress cracking, some tests and numerical simulation are carried out. Tang et al. (2016) used the finite element method to simulate the damage process of hot rock(300 ℃–600 ℃) after quenching treatment, and compared the fracture number of quenching experiments at different temperature (The quenching experiment means the experimental study on the rapid cooling of the hot rock using cryogenic fluids). Besides, the fracture length and morphology of thermal cracks were also investigated. Kumari et al. (2017) employed different method (rapid cooling and slow cooling) to cool the hot rock, combining with ARAMIS (the non-contact stress measurement system based on digital image), the strain evolution under different cooling method was analyzed. In addition, the mechanical properties and permeability of rock before and after quenching were also tested, the results showed that the rock is weakened by the rapid cooling treatment.

For the formed EGS after HDR fracturing, the heat carrying fluid will be continuously heated in the process of cryogenic fluid migration and heat transfer in fractured channel (heat exchange channel), meanwhile the hot matrix around fracture will be cooled. Then thermal stress will be produced by the temperature gradient in matrix. On one hand, the thermal stress can induce the matrix shrink when it is cold, and lead to the increase of fracture aperture. On the other hand, the thermal cracking will occur when thermal stress exceeds the rock strength. Meanwhile, a series of physical and chemical reactions will occur in fracture, which will further affect the fracture permeability. Based on the local thermal non-equilibrium model, adopting the discrete fracture network, Zhang et al. (2019a, b) investigated the promoting of thermal stress on fracture permeability during low-temperature injection. Guo et al. (2016) concluded that the heterogeneous cooling of rock mass leads to the generation of thermal stress, which leads to the shrinking of rock mass around the advantageous channel and increases the fracture opening. Pandey et al. (2017) used thin porous media layer to represent fracture and explored the permeability evolution of fracture by THM coupling simulation, the results showed that the increase in matrix permeability will enhance the matrix shrink and the opening of fracture during low-temperature fluid injection.

At present, the thermal stress/cracking involved in HDR research is mostly concentrated on the study of fracture propagation in HDR fracturing stage under thermal stress. While for heat mining stage after the formation of EGS, the damage mechanism induced by thermal stress along the fracture and its effect on fracture permeability is rarely studied. Therefore, this research conducted the 24 h permeability evolution experiment for

single fracture under high temperature to master the evolution of fracture permeability in heat mining process. Then based on meso-damage mechanics a THM-D (thermo-hydro-mechanical-damage) coupling model was established to describe the damage distribution caused by thermal cracking and further explain the evolution rule of fracture permeability during the EGS heat recovery. All in all, this study is intended to reveal the relationship between the thermal stress/cracking and the evolution of fracture permeability along EGS fracture, which can provide guidance for the prediction of EGS heat mining and the adjustment of operation parameters.

Method of permeability test

The evolution of fracture permeability in EGS is affected by numerous factors, including the confining pressure, thermal stress induced by low-temperature fluid injection and the precipitation or dissolution caused by water–rock reaction. As for the water–rock reaction is quite weak in a short period, and it takes up to several mouths to show obvious scaling, precipitation or dissolution (Zhao et al. 2020). In this study, small-scale rock samples (diameter of 0.025 m, length of 0.05 m) were used to conduct high temperature single fracture permeability tests within 24 h. Therefore, the tests ignored the water–rock reactions and focused on the effect of thermal stress/cracking on the fracture permeability evolution in heat mining process.

Experimental device

The evolution of fracture permeability determines the heat mining rate of EGS (Zhang et al. 2019a, b). So in this part the self-developed high-temperature seepage simulation device is employed to carry out the high temperature fracture permeability tests (Fig. 1). The device holds a rock sample within a constant temperature cell with imposed confining pressure (0–50 MPa). And high temperature can be controlled by oil bath (room

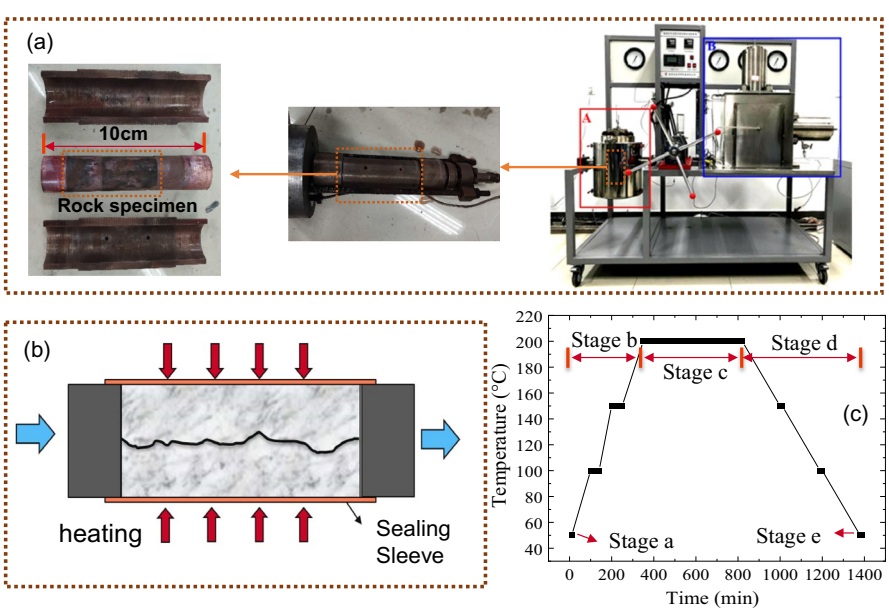

Fig. 1 Experimental device and scheme (**a** experimental device; **b** schematic diagram of the internal structure; c. experimental scheme)

temperature to 300 ℃). Fluid is injected into one end of the sample by the pump with constant flow rate. To prevent the vaporization of injection fluid under high temperature, the back pressure valve is installed at the outlet end. Based on the opening principle of hydraulic fractures is that the tensile stress acting on matrix exceeds the limit of tensile strength, we use Brazilian splitting to generate fracture on standard core in these tests.

Experimental sample

Wulian granites taken from Shandong Rizhao open-pit mine are used in these tests. The samples are prepared with the diameter of 0.025 m and the height of 0.05 m. And the basic parameters of the rock sample are as follows (Zhang et al. 2021): matrix porosity is 1.79%, matrix permeability is 0.05×10^{-15} m^2, uniaxial compressive strength is 160 MPa, and Young's modulus is 25.7 GPa. The mineral composition is 41% of quartz, 7% of potash feldspar, 30% of plagioclase, 19% of calcite, and 3% of clay minerals. The physical and mechanical properties of the sandstone used in experiments are close to those of granite, which are as follows: matrix porosity is 2.01%, matrix permeability is 0.036×10^{-15} m^2, uniaxial compressive strength is 156 MPa, and Young's modulus is 27.1 GPa. And the mineral composition of the tight sandstone is 58% of quartz, 2% of potash feldspar, 10% of plagioclase, 11% of calcite, 3% of Hematite, 4% of dolomite and 12% of clay minerals.

Experimental purpose and content

The experiment involves: a. the initial permeability test at 50 ℃; b. the permeability test at rock heating stage, from 50 ℃ → 100 ℃ → 150 ℃ → 200 ℃; c. the long-term permeability test after the temperature rise to 200 ℃; d. the permeability test when temperature drops from 200 ℃ → 150 ℃ → 100 ℃ → 50 ℃; e. the permeability test at 50 ℃ after the temperature rise and drop program. By comparing the permeability changes of stage-e and stage-a, we can infer the influence of EGS heat mining process on fracture permeability. In these tests, the fracture is closed in situ, and the effect of confining pressure, injection velocity and lithology difference on fracture permeability evolution during heat mining process is explored. The specific experimental scheme is shown in Table 1.

Experimental procedures and data processing

The experimental procedures are as follows: a. make the standard sample, dry the sample and then obtain its weight; b. fix the sample in copper sleeve and seal it with

Table 1 Experimental Scheme

Item	Rock Type	Injection velocity(mL/min)	Confining pressure	Temperature program
1	Granite	5	20	50 ℃ → (C) → 50 ℃ → (R) → 100 ℃ → (R) → 150 ℃ → (R) → 200 ℃ → (C) → 200 ℃ → (D) → 150 ℃ → (D) → 100 ℃ → (D) → 50 ℃ → (C) → 50 ℃
2	Granite	5	25	
3	Granite	10	25	
4	Sandstone	5	20	

(R) represents the temperature rising period; (C) represents the temperature constant stage; (D) represents the temperature decreasing period

the high-temperature holder combined with a graphite sealing ring; c. install the core holder into the high-temperature seepage device, connect the pipeline and check the instrument tightness; d. load the designed confining pressure; e. set the experimental temperature, then using the 20 ℃ water to measure the fracture permeability at 50 ℃, 100 ℃,150 ℃ and 200 ℃, respectively, during the heating and cooling process, and conduct long-term fracture permeability test at 200 ℃; f. to avoid fluid gasification in fracture at high temperature, set a constant pressure of 2 MPa to control the outlet pressure; g. measure the injection pressure to infer the permeability; h. unload the confining pressure and take out the sample after the instruments cool to room temperature; i. dry the sample, collect the debris particles falling off the rock surface and then obtain their weight.

Combined with the equivalent fracture aperture, the modified cubic law can be employed to describe the hydraulic characteristics of the single fracture (Eq. 1) in the permeability calculation after experiment (Shu et al. 2019). Besides, Darcy's law can still be used to calculate the fracture permeability due to the low flow rate (Eq. 2).

$$q = \frac{Pd_r b_f^3}{12\mu L} \tag{1}$$

where, q represents the injection velocity, m^3/s, which are controlled by the experiment scheme; P represents the pressure difference between inlet and outlet, Pa, which are measured in experiments; d_r represents the fracture width, which is equal to the rock diameter, m; b_f represents the fracture aperture, which is inferred based on the measured pressure, m; μrepresents the dynamic viscosity, Pa·s; L represents the fracture length, m. The dynamic viscosity at different temperature can be obtained by empirical formula (Qu et al. 2017), therefore, the equivalent fracture width b_f can be calculated by Eq. 1.

$$k_e = \frac{q\mu L}{PA} \tag{2}$$

where, k_e is the equivalent permeability, m^2; A is the fracture area, $A = d_r \cdot b_f$, m^2. The relationship between equivalent permeability k_e and equivalent fracture width b_f can be obtained from Eqs. (1) and (2), as shown in Eq. (3).

$$k_e = \frac{b_f^2}{12} \tag{3}$$

Results of permeability test

Permeability evolution of the EGS fracture under thermal stress/cracking

Since the initial difference in fracture permeability of the split specimens, to facilitate the analysis of permeability evolution under different experimental conditions, the permeability retention rate (the real time measurement value of permeability/initial value of permeability) is used to explore the evolution rule. In the test of item1, the experimental conditions can be seen in Table1, the fracture permeability decreases in the 50–150 ℃ heating stage due to the thermal expansion of matrix with the increase of rock temperature. When the rock reaches 200 ℃, the increased temperature difference between

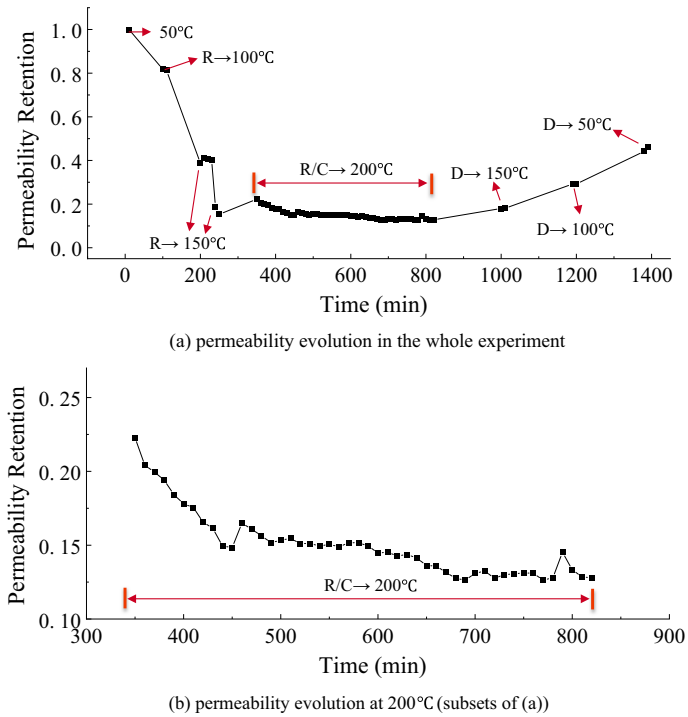

Fig. 2 Permeability evolution of the fractured EGS under the experimental condition of Item1; **a** permeability evolution in the whole experiment; **b** permeability evolution at 200 ℃ (R represents the temperature rising period; D represents the temperature decreasing period; R/C represents the temperature first rising and then remain steady)

injection fluid and hot rock enhanced the low-temperature induced thermal stress, on one hand the thermal stress can induce the matrix shrink and lead to the increase of fracture aperture, on the other hand thermal cracking emergences in matrix along fracture. So when the temperature rises to 200 ℃, in the early injection stage, the fracture permeability increases under thermal stress/cracking (Fig. 2a).

At 200 ℃, the continuous injection of heat-carrying fluid makes the temperature of fluid and rock tend to be in equilibrium. Then the reduced temperature difference makes the increment of fracture aperture caused by thermal stress begin to decrease. After the cracking period, the debris particles generated by thermal cracking will block the heat-carrying channel, resulting in the reduction of fracture permeability. This period can be called the blocking stage, as shown in Fig. 2b.

Permeability test is conducted for about 10 h at 200 ℃, then stop heating and the permeability is tested during the natural cooling process. As the weakening of matrix expansion with temperature reduction, the permeability increases. However, the fracture permeability cannot be restored to original state due to the blockage of debris particles created by thermal cracking.

Distribution of rock damage

After the series of permeability experiments under different temperatures (from stage-a to stage-d), to obtain the damage distribution around the EGS fracture, the CT scanning test is carried out using the rock specimen before and after permeability experiments.

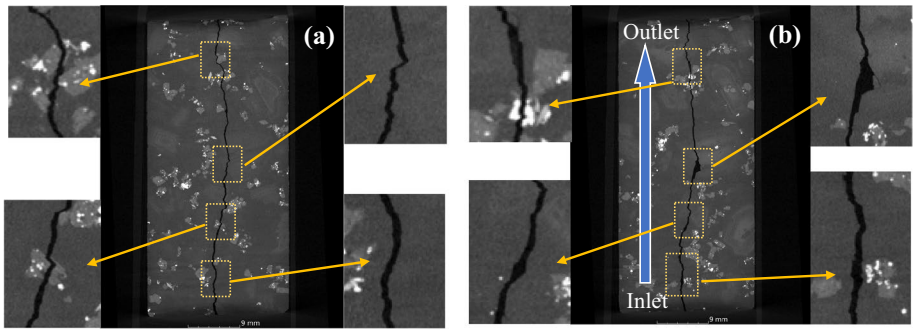

Fig. 3 Cross section of CT scanning of Item1 before (**a**) and after (**b**) high-temperature permeability experiment

As shown in Fig. 3, after high-temperature permeability experiment under the function of thermal stress/crack, the micro cracks generated along the EGS fracture, and the intensified thermal cracking emerged around the entrance part and the middle part of EGS fracture. In addition, the large gap in yellow box show the crushing area after the flooding of low-temperature fluid under thermal stress.

Influence of different factors on fracture permeability evolution

Confining pressure Keeping the other experimental conditions unchanged, at confining pressure of 25 MPa, the permeability increases by 170% when temperature arises from 150℃ to 200 ℃ (Fig. 4). While, at confining pressure of 20 MPa, the permeability increases only by 45.5% when temperature arise from 150 ℃ to 200 ℃. During the long-term permeability test at 200℃, the permeability decreases by 16.13% at the confining pressure of 25 MPa in the blocking stage, while the permeability decreases by 45.56% at the confining pressure of 20 MPa. It can be deduced that the thermal cracking is enhanced with the increase of confining pressure and raises the permeability increment in thermal cracking stage. Meanwhile, the increase of confining pressure limits the migration of debris particles, thereby reducing the tendency of blockage in blocking stage. After permeability test at 200 ℃, the temperature is reduced to 50 ℃ naturally, the permeability recovers to 74.4% when the confining pressure is 25 MPa, and it only recovers to 45.5% when the confining pressure is 20 MPa.

Injection velocity Obviously, the increase of injection velocity will raise the fluid pressure in fracture. Therefore, the increase of injection velocity in temperature rising stage (from 50 to 150 ℃) can inhibit the matrix expansion, and the permeability change at this stage is relatively small. When temperature raise to 150 ℃, the permeability decreased by about 90% at the flow velocity of 5 mL/min, and the decline is 65% at the flow velocity of 10 mL/min, as can be seen in Figs. 4 and 5.

When temperature rises to 200 ℃, the low-temperature fluid can maintain a durable low temperature state due to the increase of flow velocity, thereby obtaining the better thermal cracking effect. As shown in Fig. 5, for the flow velocity of 10 mL/min, the permeability increases for about 30 min in thermal cracking stage, which is longer than that of the flow velocity of 5 mL/min. Due to the permeability evolution of the fractured hot rock is affected by not only the micro-cracks induced by thermal cracking, the fracture

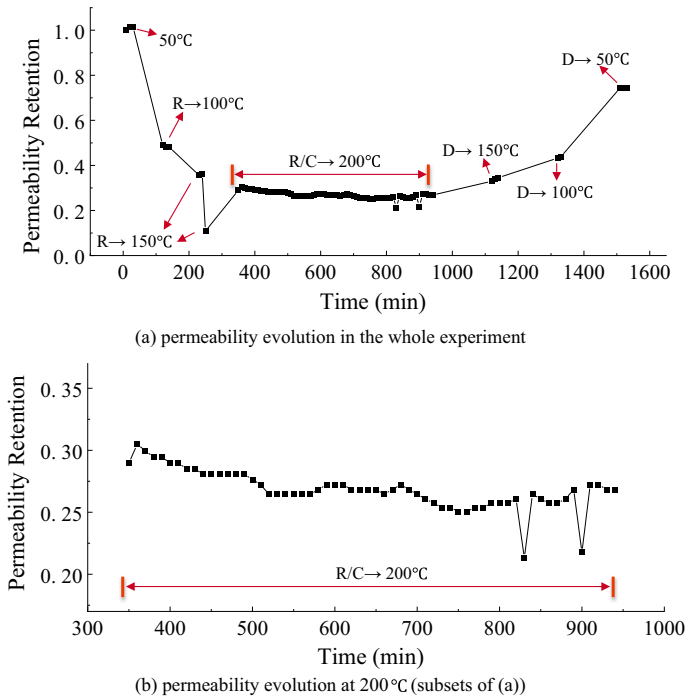

Fig. 4 Permeability evolution of the fractured EGS under the experimental condition of Item2; **a** permeability evolution in the whole experiment; **b** permeability evolution at 200 ℃ (R represents the temperature rising period; D represents the temperature decreasing period; R/C represents the temperature first rising and then remain steady)

aperture controlled by thermal stress and the injection pressure but also the debris particles generated by cracking, the blockage tendency intensifies with the increase of debris particles caused by the enhanced thermal cracking. In permeability test at 200 ℃, the permeability reduction is 20.4% when the injection velocity is 10 mL/min, while the reduction is 16.6% when that is 5 mL/min (Figs. 4 and 5). After the 200 ℃ permeability tests, when the experimental temperature drops to 50 ℃ naturally, the permeability recovery rate is 74.4% at 5 mL/min and 62.5% at 10 mL/min. After experiment, 0.163 *g* of debris particles are collected in Item3 (the flow velocity of 10 mL/min), compared with 0.124 *g* of debris particles in Item2 (the flow velocity of 5 ml/min). Therefore, it indicates again that thermal cracking is enhanced under high injection velocity, and the increase of debris particles reduces the permeability recovery rate.

Rock heterogeneity The heterogeneity of rock sample has the significance influence on thermal stress/cracking of hot rock (Zhang et al. 2019a, b). Although the hot dry rocks are dominated by granite, to clarify the permeability evolution of fractured hot rock with different lithology specimens, this part addresses the influence of the difference in heterogeneity between granite and sandstone on permeability evolution.

During temperature rising stage from 50 ℃ to 150 ℃, the permeability evolution of sandstone is almost the same as that of granite. In this period, under the thermal expansion of rock matrix, the fracture permeability decreases with the rising temperature due to fracture closure (Fig. 6a). When temperature rises to 200 ℃, firstly the permeability raises

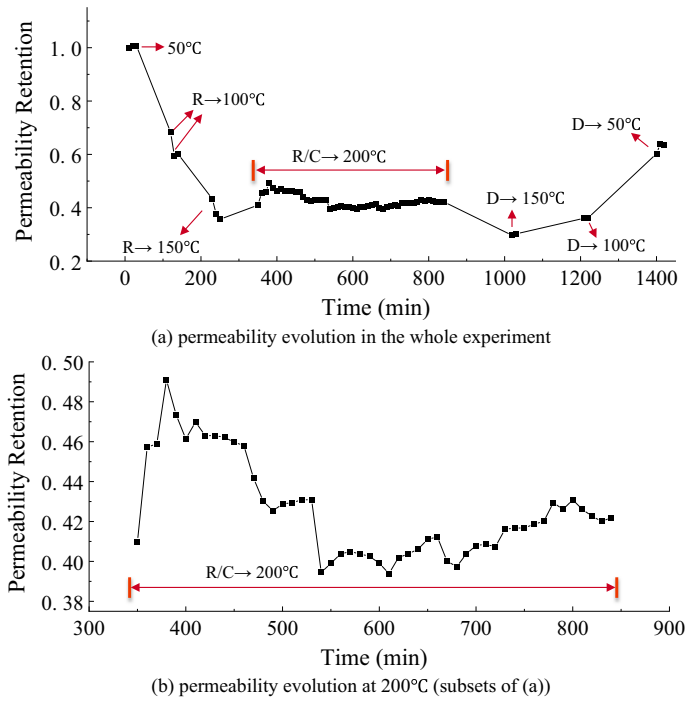

Fig. 5 Permeability evolution of the fractured EGS under the experimental condition of Item3; **a** permeability evolution in the whole experiment; **b** permeability evolution at 200 ℃ (R represents the temperature rising period; D represents the temperature decreasing period; R/C represents the temperature first rising and then remain steady)

under thermal cracking, and then decreases due to the blockage of the migration of debris particles caused by cracking. However, when permeability drops to 40% of the initial permeability, the blockage will be unblocked under the scouring of injection fluid, and the permeability returned to the initial value at 200 ℃ (Fig. 6b).

When temperature drops to 50 ℃ naturally, the permeability increases to 4.8 times of the initial state (at 50 ℃), which indicates the generation of thermal cracking during heat mining process. After experiment, 0.079 *g* of debris particles are collected, compared with 0.124 *g* of debris particles in Item2 (Fig. 7). Therefore, on one hand, the smaller amount of debris may mean that the modest thermal fracturing because of reduced heterogeneity of Item4, and on the other hand, the smaller debris particles generated in heat mining process will be easily flushed by injected water.

All in all, when using low-temperature fluid to extract heat from hot rock through fractures, the low-temperature induced thermal stress, the micro-cracks and the debris particles generated by thermal cracking will jointly affect the fracture permeability. Therefore, it is necessary to further study the relationship between thermal stress/cracking caused by temperature gradient and fracture permeability response, then to predict the permeability evolution based on the damage degree.

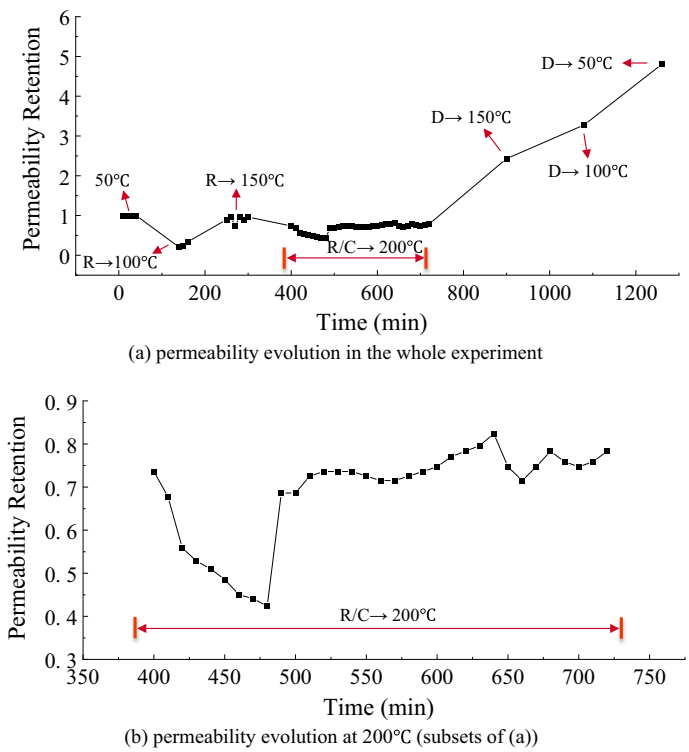

Fig. 6 Permeability evolution of the fractured EGS under the experimental condition of Item4; **a** permeability evolution in the whole experiment; **b** permeability evolution at 200 ℃ (R represents the temperature rising period; D represents the temperature decreasing period; R/C represents the temperature first rising and then remain steady)

Method of damage simulation

By the high temperature permeability test of EGS fracture we have drawn the conclusion that the fracture permeability presents the trend of first increase and then decrease, the permeability increase is induced by the thermal stress/thermal cracking (as can be seen in CT scanning results in Fig. 3), and the permeability decrease is induced by the blockage of debris particles induced by thermal cracking. Therefore, the origin of permeability evolution lies in the thermal cracking during the injection of low-temperature fluid. In this part, based on the THM-D coupling the thermal cracking research is conducted to investigate the degree and rule of damage along the EGS fracture during the injection of low-temperature fluid. Furthermore, to establish the relationship between the thermal cracking along fracture and the fracture permeability evolution.

THMD coupling model for fractured hot rock

For the thermal cracking in intact rock, the coupling model of thermo-hydro-mechanical-damage(THMD) has been described in detail in previous studies by Zhang et al. (2019a, b), including the quasi-static equilibrium equation considering the variation of pore pressure and temperature, the temperature field equation considering heat convection and stress action, the seepage field equation considering temperature and

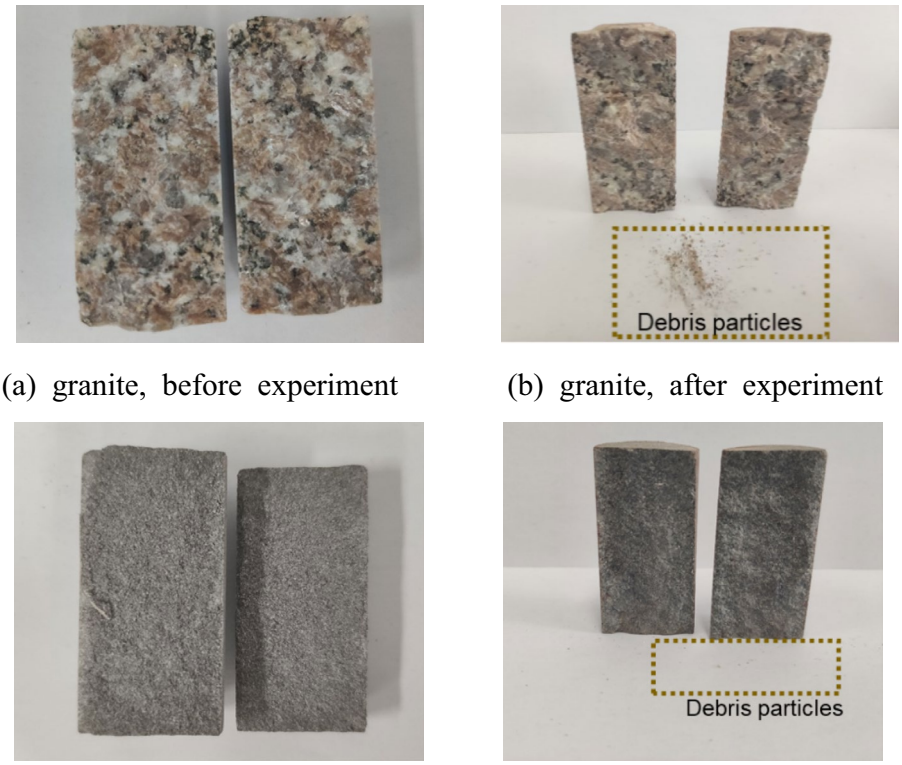

(a) granite, before experiment (b) granite, after experiment

(c) sandstone, before experiment (d) sandstone, after experiment

Fig. 7 Debris particles generated during the permeability test of fractured hot rock

stress, damage criterion and the influence degree of damage on thermal-flow-solid parameters of rock (Zhu et al. 2014; Wei et al. 2015).

In this study, the purpose is to analyze the damage propagation in fractured rock mass under thermal stress. Discrete fractures are used to describe the main fracture. Based on the THMD coupling for matrix, to explore the influence of fracture flow and heat transfer on stress filed and rock damage, it is necessary to add the governing equation of fracture flow and heat transfer to simulate the fluid flow and heat transfer in fracture. The governing equations for flow and heat transfer in fracture are as follows:

Mass conservation equation in fracture:

$$d_f \rho_f S_f \frac{\partial p}{\partial t} + \nabla_\tau \cdot (d_f \rho_f v_f) = Q_f \tag{4}$$

$$v_f = -\frac{k_f}{\mu} \nabla_\tau \cdot p \tag{5}$$

Equation (4) is the mass conservation equation in fracture. Where, d_f is the fracture width, m; ρ_f is the fracture density, kg/m^3; S_f is the water storage coefficient in fracture, Q_f is the flow exchange between matrix and fracture, kg/(m^3·s); k_f is the fracture permeability, m^2; $\nabla\tau$ is the tangential gradient along fracture; p is the pressure in fracture, Pa; μrepresents the fluid viscosity; v_f represents the fluid velocity in fracture, m/s.

Energy equation of heat conduction and convection in fracture (Qu et al. 2017):

$$d_f(\rho C)_{eff}\frac{\partial T_f}{\partial t} + d_f\rho_f C_f v \cdot \nabla_\tau T_f = Q_f + \nabla_\tau(d_f\lambda_{eff}\nabla_\tau T_f) \tag{6}$$

where, d_f is the fracture width, m; $(\rho C)_{eff}$ is the effective specific heat capacity, $(\rho C)_{eff} = \rho_s C_s(1-\phi) + \rho_w C_w \phi$, ρ_s represents the solid density (fracture) and ρ_w represents the water density, C_s represents the specific heat capacity of solid and C_w represents the specific heat capacity of water, ϕ represents the porosity of fracture; λ_{eff} is the effective heat transfer coefficient, $\lambda_{eff} = \lambda_s(1-\phi) + \lambda_w\phi$, λ_s represents the thermal conductivity of solid and λ_w represents the thermal conductivity of water; v is the fluid velocity in rock and the Darcy's law is obeyed.

The technique route of damage analysis used in this research is similar to the RFPA (a numerical calculation tool which can simulate the progressive failure of materials) developed by Professor Tang based on the meso-damage mechanics theory (Wei et al. 2015). Based on the THM-D coupling, the injection pressure and thermal stress jointly drive the evolution of stress field. And considering the material heterogeneity, the weakening treatment will be conducted for the damage elements which meet the given failure criterion. Then the failure process of the heterogeneous material can be realized numerically.

The damage factor is judged by the appropriate failure criteria. The maximum tensile stress criterion or Mohr–Coulomb criterion is adopted as the damage judgment, the tensile failure will occur when $F_1 \geq 0$, and the shear failure will occur when $F_2 \geq 0$, where:

$$F_1 = \sigma - f_t \tag{7}$$

$$F_2 = -\sigma_3 - f_c + \frac{1+\sin\varphi}{1-\sin\varphi}\sigma_1 \tag{8}$$

where, f_t is the uniaxial tensile strength, Pa; f_c is the uniaxial compressive strength, Pa;φ is the internal friction angle, °; σ_1 is the maximum principal stress, Pa; σ_3 is the minimum principal stress, Pa.

For the relationship between damage factor D and strain of elements, when $F_1 \geq 0$, the damage factor D is (Zhang et al. 2019a, b):

$$D = \begin{cases} 0 & \varepsilon < \varepsilon_{t0} \\ 1 - \frac{\lambda\varepsilon_{t0}}{\varepsilon} & \varepsilon_{t0} \leq \varepsilon < \varepsilon_{tu} \\ 1 & \varepsilon \leq \varepsilon \end{cases} \tag{9}$$

when $F_2 \geq 0$, the damage factor D is:

$$D = \begin{cases} 0 & \varepsilon_{c0} < \varepsilon \\ 1 - \frac{\lambda\varepsilon_{c0}}{\varepsilon} & \varepsilon \leq \varepsilon_{t0} \end{cases} \tag{10}$$

where, λ is the residual tensile strength coefficient, $\lambda = f_{tr}/f_{t0}$, f_{t0} and c are, respecively, the uniaxial tensile strength and residual strength; ε_{t0} is the tensile strain corresponding to the elastic limit; ε_{c0} is the compressive strain corresponding to the elastic limit;. $\varepsilon_{tu} = \eta \cdot \varepsilon_{t0}$,η is the ultimate strain coefficient.

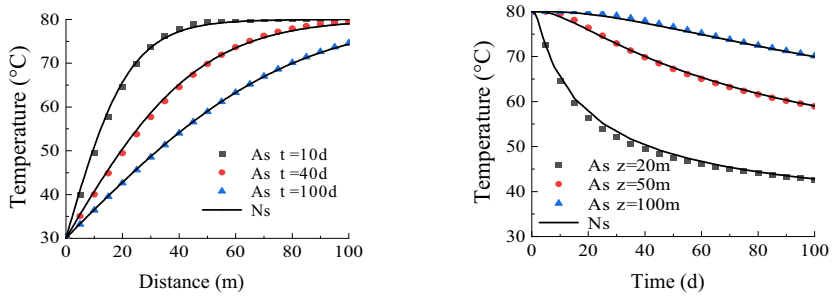

(a) temperature distribution along the single fracture (b) temperature evolution at the three point

Fig. 8 Variation of fluid temperature in fracture (As represents the analytic solution and Ns represents the numerical solution)

Model validation

For intact granite, the damage simulation based on THMD coupling model has been verified in previous research. In this paper, the influence of fracture flow and heat transfer on temperature field and the response of temperature field to stress distribution are added. For heat transfer in the single fracture, Lauwerie (1995) drawn the analytical solution of the temperature evolution in single fracture during the research on heat transfer in oil field. At the certain time, the temperature distribution in fracture along the x-axis is as follows:

$$T(x,t) = T_0 + (T_{in} - T_0)erfc\left[\frac{(\lambda_s x)/(\rho_w C_w d_f)}{2\sqrt{\lambda_s/(\rho_s C_s)u_f(u_f t - x)}}\right]U(t - x/u_f) \tag{11}$$

where, *erfc* is co-error function; U is the unit step function; u_f is the fluid velocity in fracture; T_0 is the initial temperature; T_{in} is the injection temperature.

The temperature and seepage coupling model of a single fracture is solved by fracture flow and fracture heat transfer module in COMSOL. Parameters in verification model are as follows: fluid density is 1000 kg/m^3, fluid viscosity is 1 mPa·s, fluid specific heat capacity is 4200 J/kg/K, rock density is 2700 kg/m^3, the rock specific heat capacity is 1000 J/kg/K, the thermal conductivity of matrix is 3 W/m/K, and the flow velocity in fracture is 0.02 m/s. As shown in Fig. 8, comparing the simulation results with the analytical solution, the numerical solution is basically consistent with the analytical solution, which shows that the mathematical model and calculation method in this research are feasible for the simulation of flow and heat transfer in fracture.

Geometric model and boundary conditions

The geometric model used is the same size as the experimental sample in Sect. "Method of permeability test" (0.025 m × 0.05 m), the heat-carrying fluid is injected from the model top along the fracture direction, and the fracture in model are set by discrete fracture. The specific boundary conditions are shown in Fig. 9a, the confining pressure is provided perpendicular to fracture surface, the injection temperature is T_{inj} and the initial rock temperature is T_0. The triangular mesh elements are used for mesh generation with 27,595 triangular elements and 813 edge elements, as shown in Fig. 9b. The specific

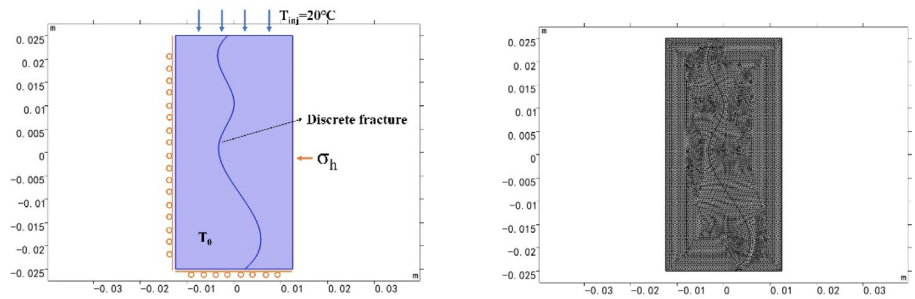

(a) model sketch and boundary conditions (b) model grid

Fig. 9 Damage simulation model of the fractured hot rock

model parameters are shown in Tables 2 and 3. Due to the damage generated by thermal stress/thermal cracking is emerged in early stage of the heat transfer between hot rock and low-temperature fluid (the temperature difference is larger in early stage of the heat transfer), the damage simulation duration always less than 10 s.

Simulation results

Evolution of damage and various physical fields in heat mining process

During the injection of low-temperature fluid into hot rock, due to the existence of main fracture generated by fracturing, the low temperature carried by injection fluid is transferred to the rock matrix along fracture, as shown in Fig. 10. The matrix around

Table 2 Parameters related to damage model (Wei et al. 2015)

Parameters	Symbol	Value	Unit
Ultimate compressive strain coefficient	ηc	150	/
Ultimate tensile strain coefficient	ηt	5	/
Thermal expansion coefficient	α_T	6×10^{-6}	1/K
Internal friction angle	θ	45	°
Tensile strength	f_t	31	MPa
Compressive strength	f_c	280	MPa
Young's modulus	E	39	GPa
Residual strength factor	λ	0.1	/
Specific heat capacity	C_m	950	J/kg/K

Table 3 Model boundary and initial condition

Parameters	Symbol	Value	Unit
Initial temperature of hot rock	T_0	200	℃
Temperature of the fracturing fluid	T_{inj}	20	℃
Injection pump rate	U_{inj}	5/10	mL/min
Heat transfer coefficient between fluid and rock	h	4000	W/(m^2 K)
Confining pressure	σ_h	20/25	MPa
Heterogeneity of physical and mechanical parameter	m	10/30	/
Fracture width	d_{fr}	1	mm
Fracture permeability	k_{fr}	3×10^{-12}	m^2
Matrix permeability	k_m	5×10^{-18}	m^2

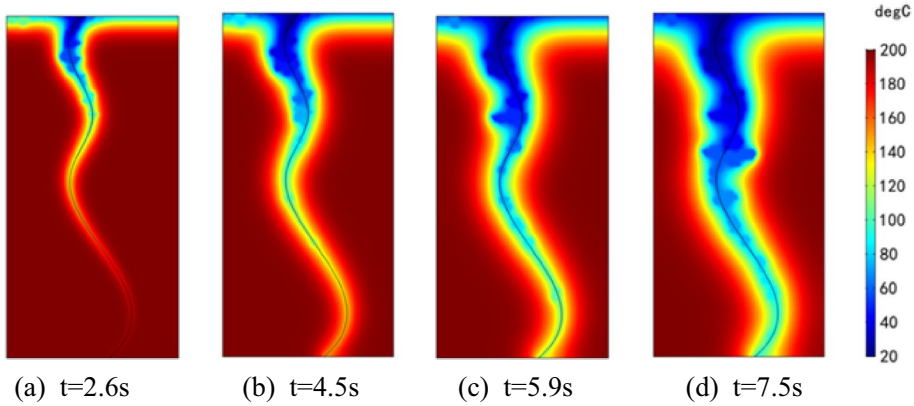

Fig. 10 Evolution of temperature field in heat mining of the fractured hot rock based on THM-D model

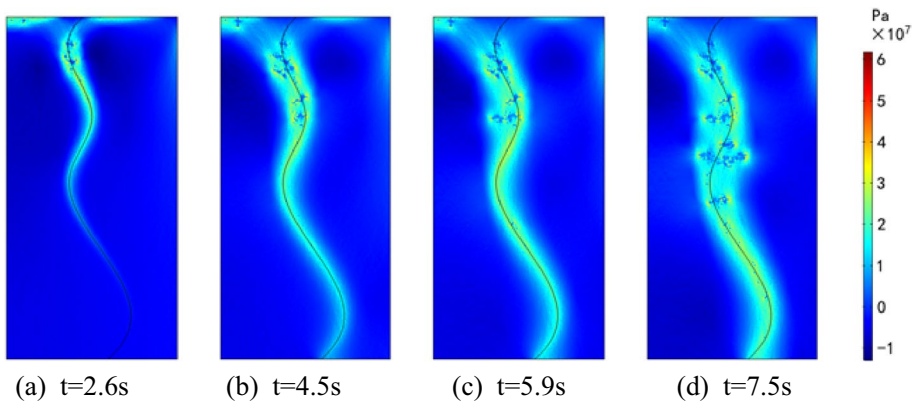

Fig. 11 Evolution of the maximum stress field in heat mining of the fractured hot rock based on THM-D model

the fracture is gradually cooled by the injection of low-temperature fluid, and the temperature of injection fluid and matrix gradually tends to be balance. Corresponding to the temperature gradient formed in matrix present a trend of first increasing and then decreasing. Similar to the thermal stress produced by the injection of low-temperature fluid around wellbore, the low-temperature induced thermal stress presents tensile stress along fracture (Zhang et al. 2019a, b). And the thermal stress controlled by the variation of temperature gradient increase first and then decrease, as shown in Fig. 11. When $t = 4.5$ s, the maximum tensile stress around fracture is 60 MPa, and the tensile stress gradually decreases with the temperature gradient tend to be stable. In addition, the concentration of tensile stress moves towards the outlet with the migration of low temperature field during the heat mining.

The reason for the formation of microcracks is that the stress concentration in matrix reaches the damage failure condition. In this research, we set the criterion of Maximum Tensile Stress and criterion of Mohr Coulomb as the damage judging condition and give priority to judging the criterion of maximum tensile stress. The damage occurs on the fracture wall, and then the crack propagates perpendicular to the main fracture. With the low temperature field moving toward the outlet, the new damage gradually forms along the flow path. The growth and propagation of thermal cracks (the generation of

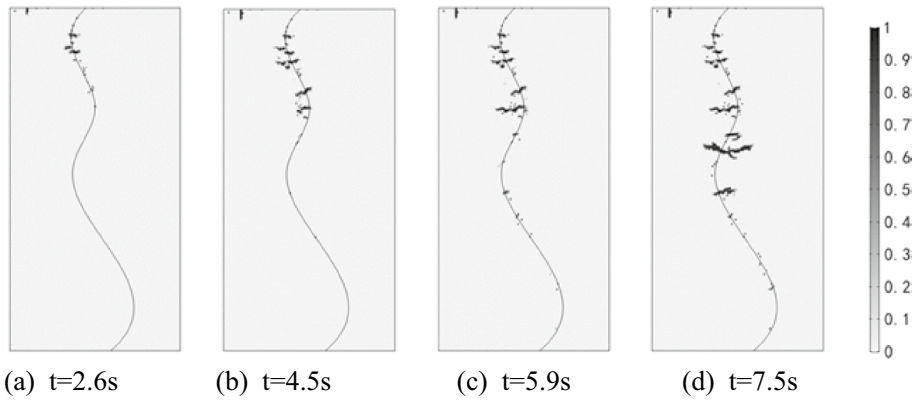

Fig. 12 Evolution of damage distribution in heat mining of the fractured hot rock based on THM-D model (the damage factor of 1 in legend represents the damage occurs and the damage factor of 0 represents no damage)

cracks caused by thermal stress) along the main fracture is shown in Fig. 12. In addition, we obtained the similar conclusion to the experiments in Sect. "Method of permeability test" that the intensified thermal cracking emerged around the entrance part and the middle part along the EGS fracture (Fig. 3).

During the injection of heat-carrying fluid, the thermal stress on matrix around fracture first increases and then decrease due to the heat exchange between fluid and rock. As the thermal stress gradually weakens with the reduction of temperature difference, the generation of thermal cracks will be suspended (Fig. 12).

Influence of injection velocity

The injection velocity of heat carrying fluid is one of the key parameters in the development of hot dry rock. Previous studies have shown that the alteration of injection velocity has an important impact on heat extraction efficiency and production temperature in EGS (Ma et al. 2020a, b). However, the permeability evolution of fracture in EGS mining process has not been considered in current research. In permeability evolution tests conducted in this study, it is concluded that the increase of injection velocity aggravates the thermal cracking and increases the number of debris particles. Meanwhile, the debris particles will migrate with heat-carrying fluid in the main fracture. Therefore, the fracture permeability shows a trend of first increasing and then decreasing.

To investigate the influence of injection velocity on thermal cracking, the velocity is set as 5 mL/min, 10 mL/min, 15 mL/min, 20 mL/min and 25 mL/min, respectively. With the increase of injection velocity, the heating rate of fluid becomes slower, and the low temperature field is transferred faster around the fracture by the low-temperature fluid. Consequently, a larger temperature gradient is formed in matrix around the main fracture, and the thermal cracking is aggravated.

When the flow rate is 10 mL/min, the generated thermal cracks increase in length and number along time. In addition, the increase in injection velocity expands the scope of cold front, and also generate a large number of cracks at the end of the rock sample. As shown in Figs. 12 and 13, when the injection velocity is 5 mL/min, the damage is almost no longer generated after 7.5 s, and the corresponding damage quantity is 6320. While

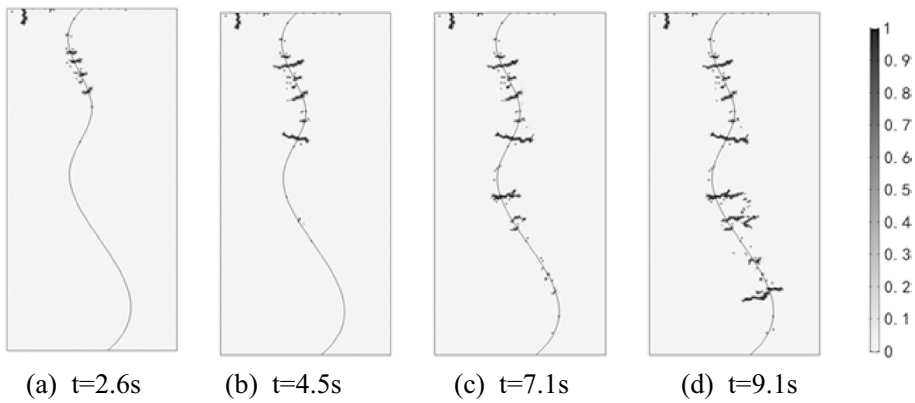

Fig. 13 Evolution of damage distribution in heat mining of the fractured hot rock with the injection velocity of 10 mL/min (the damage factor of 1 in legend represents the damage occurs and the damage factor of 0 represents no damage)

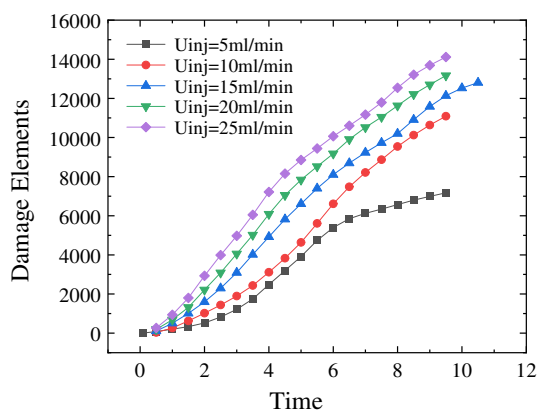

Fig. 14 Influence of the injection velocity on damage quantity (the number of damage elements means the number of elements whose value of damage factor reached to 1)

when the injection velocity is 10 mL/min, the damage quantity is 10,037 at $t = 9.1$ s (Fig. 14). And can be seen that the damage quantity will be increased with the raise of injection velocity. And the duration of thermal cracking will be prolonged with the raised injection velocity.

Influence of confining pressure

Under the in-situ stress, the main fracture in rock will close. To simplify the simulation, the confining pressure is merely applied perpendicular to the fracture direction. And the magnitude of in-situ stress will also be reflected in the confining pressure of fracture. In the experimental test of influence of confining pressure on fracture permeability evolution, it has been known that with the raise of confining pressure, the thermal cracking is intensified, which increases the fracture permeability.

Maintain the other model parameters unchanged, setting the confining pressure at 20 MPa, 25 MPa, 30 MPa, 35 MPa and 40 MPa to analyze the damage in hot matrix around fracture. As the low-temperature fluid contacts with the hot rock along fracture, the thermal stress is produced by the cold shrinkage of matrix around fracture. With

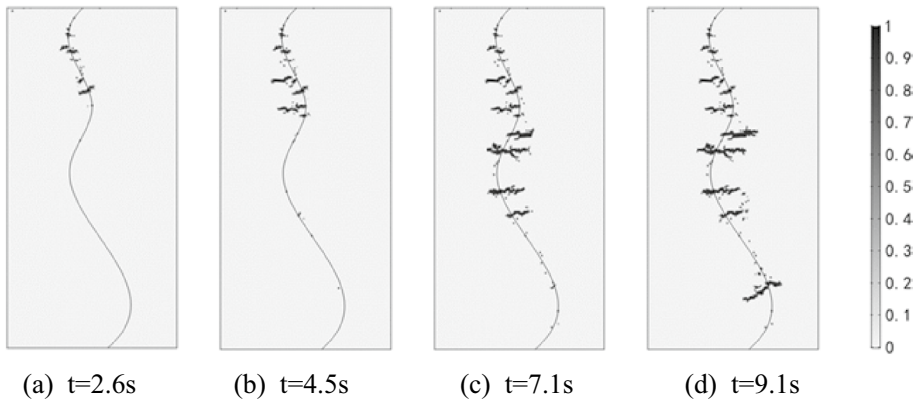

Fig. 15 Evolution of damage distribution in heat mining of the fractured hot rock with the confining pressure of 25 MPa (the damage factor of 1 in legend represents the damage occurs and the damage factor of 0 represents no damage)

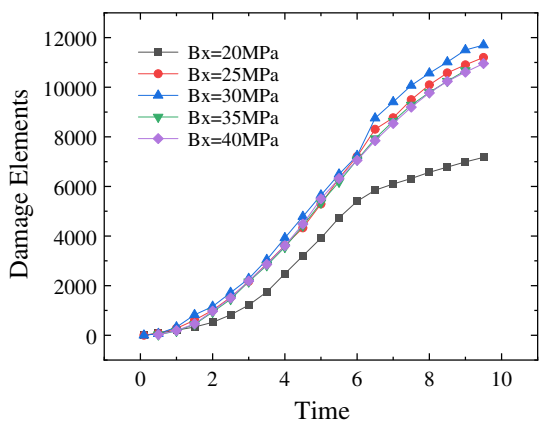

Fig. 16 Influence of the confining pressure on damage quantity (the number of damage elements means the number of elements whose value of damage factor reached to 1)

the increase of confining pressure, the maximum stress will be enhanced under thermal stress. Figure 15 shows the cracking duration will be prolonged with the confining pressure of 25 MPa, and the number and length of thermal cracks generated along the direction of confining pressure will increase. When the confining pressure is 25 MPa, the damage quantity is 11,044 at $t = 9.1$ s (Fig. 16). With the increasing of confining pressure, the stress concentration along the direction perpendicular to the original fracture is enhanced, which will promote the generation of tensile cracking. However, the increment of tensile stress comes from the thermal stress induced by temperature difference. When the confining pressure raises beyond a certain value, the heat transfer of fluid in fracture is enhanced, which decreases the temperature difference and weaken the thermal stress. Therefore, with the increase of confining pressure, the number of damage cracks increases first and then decreases.

Influence of matrix heterogeneity

Based on the meso damage theory, the numerical simulation of damage propagation in matrix around the fracture of EGS is carried out. To describe the heterogeneity of

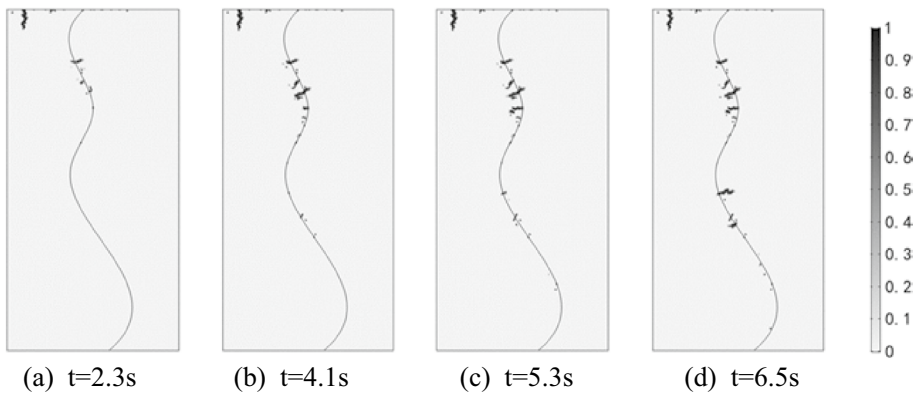

Fig. 17 Evolution of damage distribution in heat mining of the fractured hot rock with the heterogeneity coefficient of m = 30 (the damage factor of 1 in legend represents the damage occurs and the damage factor of 0 represents no damage)

material properties, it is considered that the meso element properties of rock satisfy Weibull distribution, and the following function is used (Tang et al. 2016):

$$f(u) = \frac{m}{u_0}\left(\frac{u}{u_0}\right)^{m-1} \exp\left[-\left(\frac{u}{u_0}\right)^{m}\right] \tag{12}$$

where, u represents the numerical value satisfying the distribution parameter, specifically referring to the physical and mechanical parameters of rock; u_0 is a parameter related to the average of all element parameters. The shape parameter m defines the shape of density function of Weibull distribution. We describe u_0 and m as the Weibull distribution parameter.

The mineral particles in rock are non-uniformly distributed. Previous studies have revealed that there are two kinds of microcracks in the process of thermal loading: one is the thermal cycle crack, the other is the thermal gradient crack (Zhang et al. 2019a, b). As can be seen from Fig. 12 and Fig. 17, when the matrix temperature is 200 ℃, the enhance of rock heterogeneity will promote the non-uniform expansion/ contraction of rock particles induced by temperature difference.

To investigate the influence of matrix heterogeneity on thermal cracking, the heterogeneity coefficient is set as $m = 10$, $m = 20$, $m = 30$ and $m = 40$, respectively. When the heterogeneity coefficient greater than $m = 30$, stress concentration caused by the non-uniform expansion/ contraction is weak due to low heterogeneity, so the thermal cracking perpendicular to main fracture rarely occurs, and the duration of thermal cracking is shorter. As shown in Figs. 17 and 18, the thermal cracking almost does not occur after 6.5 s.

The simulation results in this part give further explanation on the experimental phenomenon in experiment test of the influence of rock heterogeneity on fracture permeability evolution. Compared with granite, the lower heterogeneity of sandstone leads to weaker thermal cracking. Meanwhile, it generates fewer particles during the injection of low-temperature fluid and reduces the probability of particle blocking.

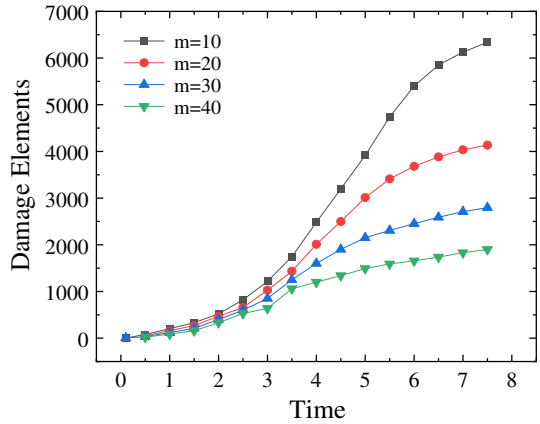

Fig. 18 Influence of the heterogeneity coefficient on damage quantity (the number of damage elements means the number of elements whose value of damage factor reached to 1)

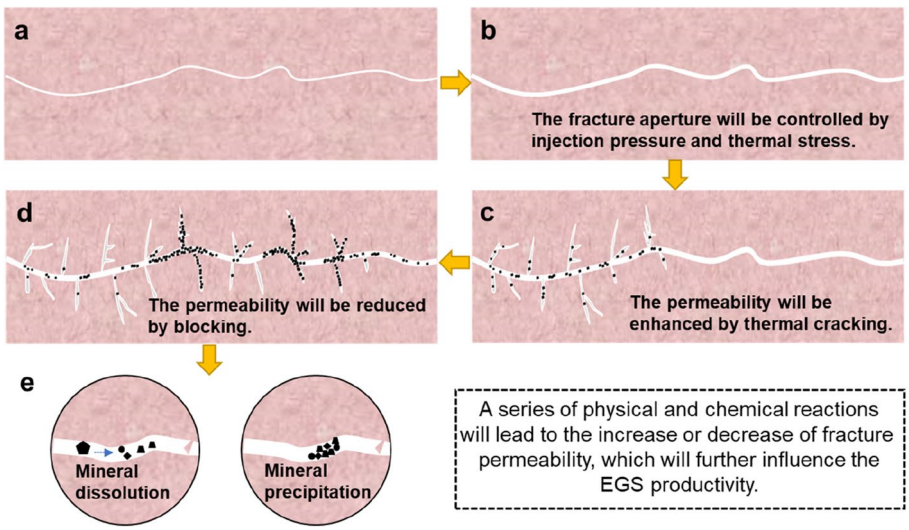

Fig. 19 Relation of thermal stress/cracking and fracture permeability evolution

Discussion

During the injection of low-temperature heat-carrying fluid, the low-temperature induced thermal stress on matrix present the trend of first increasing and then decreasing. And the effect of thermal stress is mainly divided into two aspect, ① the matrix around fracture shrinks when it is cold, which raise the fracture aperture (Fig. 19b); ② under the combination of thermal stress and injection pressure, when the maximum principal stress exceeds the rock tensile strength, thermal cracks (the generation of cracks caused by thermal stress) are formed perpendicular to main fracture, meanwhile debris particles are generated (Fig. 19c). In this stage, the thermal stress/cracking is reflected in permeability evolution as an increase in permeability (Figs. 3, 4, 5, 6). As the temperature of injection fluid and matrix tends to be balance, the thermal stress gradually weakens. However, the debris particles generated in thermal cracking will be blocked in main fracture or micro cracks with the carrying of injection fluid (Fig. 19d),

which shows that the permeability decreases continuously and finally tends to be stable (Figs. 3, 4, 5, 6). As a matter of fact, the development operation of EGS is usually several decades. The long-term water–rock interaction between heat-carrying fluid and high temperature rock will also cause mineral dissolution and precipitation (Fig. 19e), and further affect the fracture permeability.

The temperature rise and drop program in experiment is shown in Fig. 2c. At the beginning, the fracture permeability at 50 ℃ is tested (stage-a). To simulate the high-temperature characteristic of HDR, the specimen is heated from 50 ℃ to 200 ℃ in lab experiments (stage-b). And we controlled the heating rate to make the specimen almost free of thermal cracking induced by temperature increase in heating process. The long-term permeability test was then carried out at the temperature of 200 ℃ (stage-c), which corresponding to the EGS heat mining process. After the high temperature permeability experiments, the natural cooling method is used to cool the hot rock, and the fracture permeability is still monitored in this process (stage-d). Lastly, when the specimen dropped to 50 ℃ after the temperature rise and drop program, the permeability test was conducted at 50 ℃ again. Comparing with the initial permeability and resultant permeability, it was inferred that the EGS heat mining process has influences on fracture permeability. Subsequently, we draw the conclusion that the fracture permeability cannot be restored to original state due to the blockage of debris particles created by thermal cracking.

For the real EGS, more attention will be paid to the heat mining stage (stage-b). In heat mining stage, as main heat transfer channel of EGS, the evolution of hydraulic conductivity in fracture is significance for efficient heat mining. Besides, due to the temperature difference of heat carrying fluid and hot rock, the thermal stress/cracking will inevitably generate around the fracture (Avanthi et al. 2020; Gee et al. 2021; Kumari et al. 2019). So, by reveal of the relationship of thermal stress/cracking and fracture permeability evolution, the prediction of fracture permeability can be realized by the analysis of thermal stress or thermal cracking. Meanwhile, the EGS heat mining capacity can be forecasted more reasonable. Furthermore, the heat mining rate can also be optimized by the change of operation parameters.

Conclusion

This research focused on the permeability evolution and damage mechanism along the EGS fracture in heat mining stage under thermal stress/cracking, the permeability tests of high temperature rock with a single fracture were conducted to explore the permeability evolution rules, and the thermo-hydro-mechanical-damage coupling model was established to describe the damage evolution in matrix around the main fracture. Through the above research, the relationship between thermal stress/cracking and permeability evolution of hot rock with a single fracture will be concluded. The results show that:

(1) when low-temperature fluid mines heat from the high temperature fractured rock, the thermal stress or thermal cracking induced by temperature gradient and the debris particles generated by cracking will all affect the fracture permeability. Low-temperature induced thermal stress on the fractured rock can make the matrix

shrink and increase the fracture aperture. Micro-cracks generated by thermal cracking can provide channels for the migration of heat-carrying fluid. Debris particles generated during the cracking of micro-cracks can cause blockage in main fracture.

(2) During the high temperature permeability tests, the permeability first increased rapidly under thermal stress/cracking, and then decreasing due to the blockage of main fracture by debris particles caused by thermal cracking. After high temperature tests, the temperature was gradually reduced to room temperature, and the permeability cannot be restored to the initial stage due to the blockage of debris particles caused by thermal cracking.

(3) With the increase of confining pressure, the number of damage cracks increases first and then decreases. Meanwhile, the raised confining pressure limit the migration of debris particles, thus reducing the blockage probability in main fracture. Corresponding to cooling to room temperature after high temperature permeability tests, when the confining pressure is 25 MPa, the permeability recovers to 74.4%, and when the confining pressure is 20 MPa, the permeability only recovers to 45.5%.

(4) When the low-temperature fluid flows in the single fracture of hot rock, the low-temperature fluid can maintain a longer low temperature state due to the increase of flow velocity, thus obtaining a better thermal cracking effect. When the injection velocity is 5 mL/min, the damage quantity is 6320, while when the injection velocity is 10 mL/min, the damage quantity is 10,037.

(5) The low heterogeneity of rock matrix produces weak thermal cracking. There are fewer debris particles generated during heat mining process, which reduces the tendency of particle blockage. Compared with sandstone, it is more prone to form the blockage in granite during heat mining process and reduces the fracture permeability.

This study explored the permeability evolution of the fractured hot rock under thermal stress/cracking in EGS heat mining stage through long-term high temperature permeability experiments. And based on the THM-D coupling, the meso damage mechanism around the main fracture in heat mining stage is revealed. Then the relationship between the thermal stress/cracking and the evolution of fracture permeability is obtained. In next step, the mechanism of water–rock reaction and its influence on fracture permeability will be investigated. Furthermore, more effective guidance for the prediction of heat mining rate and the adjustment of operation parameters in EGS can be supplied.

Acknowledgements

This research was supported by the National Natural Science Foundation of China (42102338); China Postdoctoral Science Foundation (2022M712210); Natural Science Foundation of Shandong Province (ZR2020QE115); the Fundamental Research Funds for the Central Universities(27R1902010A); the Opening Fund of Key Laboratory of Unconventional Oil & Gas Development (China University of Petroleum (East China)), Ministry of Education.

Author contributions

WZ: conceptualization, software, data curation, formal analysis, writing—original draft, writing- review& editing. DW: data curation, formal analysis, writing- original draft. ZW: resources, methodology. TG: formal analysis, investigation, Writing—review& editing. CW: validation, resources, supervision. JH: resources, validation. LZ: resources, validation. PZ: investigation, writing—review& editing. ZQ: supervision, methodology.

Funding

National Natural Science Foundation of China (42102338); China Postdoctoral Science Foundation (2022M712210); Natural Science Foundation of Shandong Province (ZR2020QE115); the Fundamental Research Funds for the Central Universities(27R1902010A); the Opening Fund of Key Laboratory of Unconventional Oil & Gas Development (China University of Petroleum (East China)), Ministry of Education.

Availability of data and materials
The datasets used or analyzed during the current study are available from the corresponding author on reasonable request.

Declarations

Competing interests
No conflict of interest exits in the submission of this manuscript, and manuscript is approved by all authors for publication. The manuscript has not been previously published, and is not currently submitted for review to any other journal, and will not be submitted elsewhere before a decision is made by this journal.

Received: 27 May 2022 Accepted: 22 October 2023
Published online: 08 November 2023

References

Avanthi Isaka BL, Ranjith PG. Investigation of temperature- and pressure-dependent flow characteristics of supercritical carbon dioxide- induced fractures in Harcourt granite: application to CO_2-based enhanced geothermal systems. Int J Heat Mass Transf. 2020;158:119931.
Avanthi Isaka BL, Ranjith PG, Rathnaweera TD, et al. Influence of long-term operation of supercritical carbon dioxide based enhanced geothermal system on mineralogical and microstructurally-induced mechanical alteration of surrounding rock mass. Renew Energy. 2019;136:428–41.
Bongole K, Sun ZX, Yao J. Potential for geothermal heat mining by analysis of the numerical simulation parameters in proposing enhanced geothermal system at bongor basin, chad. Simul Model Pract Theory. 2021;107:102218.
Bujakowski W, Barbacki A, Miecznik M, et al. Modeling geothermal and operating parameters of EGS installations in the lower triassic sedimentary formations of the central Poland area. Renew Energy. 2015;80:441–53.
César RC, José LG, María EM, et al. Enhanced geothermal systems in Europe: an estimation and comparison of the technical and sustainable potentials. Energy. 2014;65:250–63.
Gee B, Gracie R, Dusseault MB. Multiscale short-circuiting mechanisms in multiple fracture enhanced geothermal systems. Geothermics. 2021;94:102094.
Guo B, Fu PC, Hao Y, et al. Thermal drawdown-induced flow channeling in a single fracture in EGS. Geothermics. 2016;61:46–62.
Guo TK, Tang SJ, Sun J, et al. A coupled thermal-hydraulic-mechanical modeling and evaluation of geothermal extraction in the enhanced geothermal system based on analytic hierarchy process and fuzzy comprehensive evaluation. Appl Energy. 2020;258:113981.
Hofmann H, Weides S, Babadagli T, et al. Potential for enhanced geothermal systems in Alberta, Canada. Energy. 2014a;69:578–91.
Hofmann H, Babadagli T, Zimmermann G. Hot water generation for oil sands processing from enhanced geothermal systems: process simulation for different hydraulic fracturing scenarios. Appl Energy. 2014b;113:524–47.
Huang ZW, Zhang SK, Yang RY, et al. A review of liquid nitrogen fracturing technology. Fuel. 2020;266:117040.
Jeanne P, Rutqvist J, Dobson PF, et al. The impacts of mechanical stress transfers caused by hydromechanical and thermal processes on fault stability during hydraulic stimulation in a deep geothermal reservoir. Int J Rock Mech Min Sci. 2014;72:149–63.
Jiang FM, Chen J, Huang W, et al. A three-dimensional transient model for EGS subsurface thermo-hydraulic process. Energy. 2014;72(7):300–10.
Kumari WGP, Ranjith PG. Sustainable development of enhanced geothermal systems based on geotechnical research—a review. Earth Sci Rev. 2019;199:102955.
Kumari WGP, Ranjith PG, Perera MSA, et al. Temperature-dependent mechanical behavior of Australian Strathbogie granite with different cooling treatments. Eng Geol. 2017;229:31–44.
Kumari WGP, Ranjith PG, Perera MSA, et al. Hydraulic fracturing under high temperature and pressure conditions with micro CT applications: geothermal energy from hot dry rocks. Fuel. 2018;230:138–54.
Lauwerier HA. The transport of heat in an oil layer caused by the injection of hot fluid. Appl Sci Res. 1995;5:145–50.
Li Z, Arno Z. Laboratory hydraulic fracturing experiments on crystalline rock for geothermal purposes. Earth Sci Rev. 2021;216:103580.
Li R, Huang ZW, Wu XG, et al. Cryogenic quenching of rock using liquid nitrogen as a coolant: investigation of surface effects. Int J Heat Mass Transf. 2018;119:446–59.
Ma YY, Li SB, Zhang LG, et al. Study on the effect of well layout schemes and fracture parameters on the heat extraction performance of enhanced geothermal system in fractured reservoir. Energy. 2020a;202:117811.
Ma YY, Li SB, Zhang LG, et al. Analysis on the heat extraction performance of multi-well injection enhanced geothermal system based on leaf-like bifurcated fracture networks. Energy. 2020b;213:118990.
Nadimi S, Forbes B, Moore J, et al. Effect of natural fractures on determining closure pressure. J Petrol Explor Prod Technol. 2020;10:711–28.
Pandey SN, Chaudhuri A, Kelkar S. A coupled thermo-hydro-mechanical modeling of fracture aperture alteration and reservoir deformation during heat extraction from a geothermal reservoir. Geothermics. 2017;65:17–31.
Qu ZQ, Zhang W, Guo TK. Influence of different fracture morphology on heat mining performance of enhanced geothermal systems based on COMSOL. Int J Hydrogen Energy. 2017;42:18263–78.
Sheng M, Li P, Zhuang XY, et al. Influence of cyclic normal stress on shear friction of EGS granite fractures. Eng Fract Mech. 2020;238:107268.

Shu B, Zhu RJ, Tan JQ, et al. Evolution of permeability in a single granite fracture at high temperature. Fuel. 2019;242:12–22.
Tang SB, Zhang H, Tang CA, et al. Numerical model for the cracking behavior of heterogeneous brittle solids subjected to thermal shock. Int J Solids Struct. 2016;80:520–31.
Wei CH, Zhu WC, Yu QL, et al. Numerical simulation of excavation damaged zone under coupled thermal–mechanical conditions with varying mechanical parameters. Int J Rock Mech Min Sci. 2015;75:169–81.
Xin SL, Liang HB, Hu B, et al. A 400 kW geothermal power generator using co-produced fluids from Huabei oilfield. Geotherm Resour Counc Trans. 2012;36:219–23.
Xiong Y, Fakcharoenphol P, Winterfeld P, et al. Coupled geomechanical and reactive geochemical model for fluid and heat flow: application for enhanced geothermal reservoir. SPE165982, 2013.
Zeng YC, Wu NY, Su Z, et al. Numerical simulation of heat production potential from hot dry rock by water circulating through a novel single vertical fracture at Desert Peak geothermal field. Energy. 2013;63:268–82.
Zhang YJ, Guo LL, Li ZW, et al. Electricity generation and heating potential from enhanced geothermal system in Songliao Basin, China: different reservoir stimulation strategies for tight rock and naturally fractured formations. Energy. 2015;93:1860–85.
Zhang W, Qu ZQ, Guo TK, et al. Study of the enhanced geothermal system (EGS) heat mining from variably fractured hot dry rock under thermal stress. Renew Energy. 2019a;143:855–71.
Zhang W, Guo TK, Qu ZQ, et al. Research of fracture initiation and propagation in HDR fracturing under thermal stress from meso-damage perspective. Energy. 2019b;178:508–21.
Zhang W, Wang CG, Guo TK, et al. Study on the cracking mechanism of hydraulic and supercritical CO_2 fracturing in hot dry rock under thermal stress. Energy. 2021;221:119886.
Zhao YS, Feng ZJ, Feng ZC, et al. THM (thermo-hydro-mechanical) coupled mathematical model of fractured media and numerical simulation of a 3D enhanced geothermal system at 573K and buried depth 6000–7000M. Energy. 2015;82:193–205.
Zhao YH, Feng B, Zhang GB, et al. Study of the interaction between the granitic hot dry rock (HDR) and different injection waters. Acta Geol Sin. 2020;94(7):2115–23.
Zhu WC, Wei J, Zhao J, et al. 2D numerical simulation on excavation damaged zone induced by dynamic stress redistribution. Tunn Undergr Space Technol. 2014;43(7):315–26.
Zinsalo JM, Lamarche L, Raymond J, et al. Sustainable electricity generation from an enhanced geothermal system considering reservoir heterogeneity and water losses with a discrete fractures model. Appl Therm Eng. 2021;192:116886.

Publisher's Note